OPTICAL HAROCHE AND HANLE RESONANCES

Wilhelmus M. RUYTEN
Center for Laser Applications, University of Tennessee Space Institute, Tullahoma, TN 37388, USA

Received 28 December 1989

It is shown that Haroche and Hanle resonances, known from magnetic resonance, should be observable in an optical resonance experiment in which a narrowband, phase-modulated laser resonantly excites a two-level system. The narrow Haroche resonances should allow the first observation of an optical Bloch–Siegert shift, and may find applications in modulation spectroscopy.

1. Introduction

From their inception, optical resonance experiments have followed in the steps of their magnetic predecessors. For example, Rabi oscillations, free induction decay, and spin echoes were first studied in magnetic systems. In some cases, analogies between magnetic and optical resonance are formally known, but the optical effects have not been accessible to experimental confirmation. This is the case for the Bloch-Siegert shift, which results from a counter-rotating term in the Bloch equations. For a monochromatic optical wave interacting with a two-level atom, this shift is so small that, probably, it will never be observed. Recently, however, we showed that, within the rotating wave approximation, the concept of a Bloch–Siegert shift applies to the interaction of a fully amplitude modulated field with a two-level atom [1], by straightforward analogy with a longitudinally pumped magnetic resonance experiment. This analogy allows an elegant explanation of the heuristically classified subharmonic resonance behavior of the optically driven system, namely in terms of multiple quantum resonances and their associated Bloch–Siegert-type shifts. As we also briefly pointed out, just as magnetic resonance involving transverse pumping is complementary to longitudinal pumping in many regards, so is phase-modulation complimentary to amplitude-modulation in the optical regime [2]. Here we show that, in particular, resonant excitation of a two-level atom by a phase-modulated, narrowband laser should allow the observation of optical Hanle and Haroche resonances, two types of level-crossing resonances known from magnetic resonance [3–7]. Also, we calculate that, using recent advances in phase-modulation technology, it should be possible to observe, for the first time, a small-field Bloch–Siegert-type shift in the optical regime. These new optical features are not only interesting from a fundamental standpoint, but may, perhaps, find applications in the fields of phase- and frequency-modulation spectroscopy.

2. Magnetic and optical Bloch–Siegert shifts

Consider, first, the Bloch equations for the magnetization $\boldsymbol{M}$ of a spin-1/2 system subjected to a magnetic field $\boldsymbol{H}$ and a circularly polarized light beam, propagating along the $\hat{3}$-axis (fig. 1), with associated optical pumping rate Λ_{mag} [6]:

$$\mathrm{d}\boldsymbol{M}/\mathrm{d}t=-\boldsymbol{\Gamma}\boldsymbol{M}+\gamma\boldsymbol{M}\times\boldsymbol{H}+\Lambda_{\mathrm{mag}}\hat{\boldsymbol{e}}_3 . \tag{1}$$

Here, $\boldsymbol{\Gamma}$ is a diagonal damping matrix, and γ is the gyromagnetic ratio of the magnetic doublet. Of the many possible magnetic field configurations, the longitudinal and transverse geometries have received the most attention. In both, an oscillating radiofrequency (rf) field $\boldsymbol{H}_{\mathrm{rf}}$ is applied perpendicular to a static Zeeman field $\boldsymbol{H}_0$, which is either longitudinal or transverse to the optical pumping beam (fig. 1). Thus, the magnetic "torque" $\boldsymbol{R}_{\mathrm{mag}}\equiv-\gamma\boldsymbol{H}$ is given by

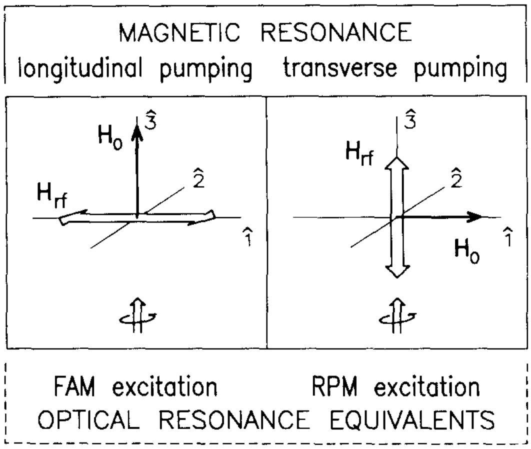

Fig. 1. Magnetic resonance geometries, whose optical counterparts are as indicated (FAM = fully amplitude modulated; RPM = resonant phase modulated).

$$\boldsymbol{R}^{\parallel}_{\text{mag}} = (\omega_{\text{rf}} \cos \Omega t, 0, \omega_0) , \tag{2}$$

or

$$\boldsymbol{R}^{\perp}_{\text{mag}} = (\omega_0, 0, \omega_{\text{rf}} \cos \Omega t) , \tag{3}$$

respectively, where Ω is the frequency of the rf field, and $\omega_0 = \gamma H_0$ and $\omega_{\text{rf}} = \gamma H_{\text{rf}}$ are the Rabi frequencies associated with the static and rf fields, respectively. The two geometries are characterized by odd and even resonances, respectively. That is, for weak rf fields, resonances occur when ω_0 is an odd (even) multiple of Ω, and the corresponding transitions can be attributed to the absorption of an odd (even) number of real (virtual) rf photons [1,4]. As the rf amplitude increases, the resonances shift and eventually disappear. These shifts are known as Bloch-Siegert shifts and have been calculated by many authors [4–8]. For example, to lowest order, the shifts of the resonances in the time-averaged fluorescence or absorption signals are given by

$$\omega_0 = N\Omega[1 - a_N(\omega_{\text{rf}}/4\Omega)^2] , \tag{4}$$

where $a_1 = 1$ for the single quantum resonance, and $a_N = 4/(N^2 - 1)$ for photon numbers $N > 1$ [5]. Apart from their parities, odd and even resonances differ in another important regard, namely their power broadening: Whereas the widths of the odd-N resonances vary as the Nth power of the rf amplitude ω_{rf}, the even-N resonances are unbroadened to lowest order in the rf amplitudes, and their associated Bloch-Siegert shifts can be measured even for weak rf fields [4–6]. The latter are the so-called Haroche resonances. In the transverse pumping geometry, there is also a resonance at $\omega_0 = 0$. This is the zero-field crossing resonance or Hanle resonance, and has been interpreted as giving rise to the dressing of the atomic Landé factor by the rf field, according to $g_{\text{rf}} = g_0 J_0(\omega_{\text{rf}}/\Omega)$, where J_0 is the zeroth-order Bessel function [4].

Consider now an optical resonance experiment on a two-level atom. The optical Bloch equations can be written as in eqs. (1), by introducing the Bloch vector $\boldsymbol{\Phi} = (u, v, w)$, whose components, respectively, are the real and imaginary parts of the atomic polarization and the population inversion [9]:

$$\mathrm{d}\boldsymbol{\Phi}/\mathrm{d}t = -\boldsymbol{\Gamma}\boldsymbol{\Phi} + \boldsymbol{R}_{\text{opt}} \times \boldsymbol{\Phi} + \Lambda_{\text{opt}} \hat{\boldsymbol{e}}_3 . \tag{5}$$

Here, Λ_{opt} is the scaled equilibrium inversion and, again, $\boldsymbol{\Gamma}$ is a diagonal damping matrix. The optical "torque" $\boldsymbol{R}_{\text{opt}}$ depends on the driving field and the frame in which eq. (5) is expressed. For example, for a constant, monochromatic field $E^{\text{C}}(t) = 2\mathscr{E} \cos \omega t$, and a frame that rotates at the two-level transition frequency ω_{12}, $\boldsymbol{R}_{\text{opt}}$ is given, exactly, by

$$\boldsymbol{R}^{\text{C}}_{\text{opt}} = (-2\kappa\mathscr{E} \cos \omega t, 0, \omega_{12}) , \tag{6}$$

where κ is the dipole coupling constant. Eqs. (2) and (6) are fully equivalent. Indeed, by substituting the appropriate variables, this equivalence leads, with $N = 1$ in eq. (4), to the conventional optical Bloch–Siegert shift, namely $\Delta = \omega_{12} - \omega = -(\kappa\mathscr{E})^2/4\omega$ [9]. Recently we showed that another equivalent interaction is that of a two-level atom driven by a fully amplitude modulated (FAM) field [2], $E^{\text{FAM}}(t) = 2\mathscr{E} \cos \Omega t \cos \omega t$. Indeed, in a frame rotating at the detuning $\Delta = \omega_{12} - \omega$, the torque $\boldsymbol{R}_{\text{opt}}$ for this interaction is given by

$$\tilde{\boldsymbol{R}}^{\text{FAM}}_{\text{opt}} = (-\kappa\mathscr{E} \cos \Omega t, 0, \Delta) , \tag{7}$$

where Ω is the modulation frequency, and where the tilde indicates that the rotating wave approximation (RWA) has been made. The multiple quantum resonances associated with this FAM interaction have been observed experimentally by Chakmakjian et al., namely in the time-averaged fluorescence from a beam of sodium atoms [10]. Because these authors studied the resonances for small detunings ($|\Delta| \leqslant \Omega$) and relatively large fields ($\kappa\mathscr{E} \geqslant \Omega$), they used the term "subharmonic resonances" rather than "multiple quantum resonances": For zero detuning and zero damping, the time-averaged fluorescence signal has maxima for modulation frequencies Ω that are subharmonics of the Rabi frequency $\kappa\mathscr{E}$, namely, for $\Omega = x\mathscr{E}/x_{0n}$, where the x_{0n}'s are the zeros of the J_0-Bessel function. Fig. 2 shows that multiple quantum resonances and subharmonic resonances are the limiting behaviors of the same resonance structures, and, in both magnetic and optical resonance, the shifts of the resonances from the weak-field values have been termed generalized Bloch–Siegert shifts [1,5,8].

Experimental verification of the conventional optical Bloch–Siegert shift, namely that associated with eq. (6), is improbable because for the super-intense fields necessary to produce a Rabi frequency $\kappa\mathscr{E}$ on the order of the optical frequency ω, the two-level approximation is no longer valid [9]. Similarly, for the FAM interaction studied by Chakmakjian et al., measurement of the weak-field Bloch-Siegert shifts is complicated by the power broadening of the odd-N resonances. Nevertheless, we contend that measurement of the weak-field Bloch-Siegert shifts from eq. (4) should be possible in an optical resonance experiment, namely one in which the FAM field is replaced by a resonant phase-modulated (RPM) field of the form

$$E^{\mathrm{RPM}}(t) = 2\mathscr{E} \cos(\omega_{12} t - M \sin \Omega t) , \tag{8}$$

where, again, Ω is the modulation frequency, and M is the modulation index. In a frame rotating at the instantaneous frequency of the RPM field, the optical torque associated with eq. (8) becomes

$$\tilde{\boldsymbol{R}}_{\mathrm{opt}}^{\mathrm{RPM}} = (-\kappa\mathscr{E}, 0, M\Omega \cos \Omega t) , \tag{9}$$

where, as for the FAM case, the RWA has been made, and the detuning Δ has been set to zero. Comparison of eq. (9) with eq. (3) shows that this RPM interaction is the optical equivalent of a transversely pumped magnetic resonance experiment. Therefore it should display the narrow, even-N, Haroche resonances, as well as the zero-field Hanle resonances.

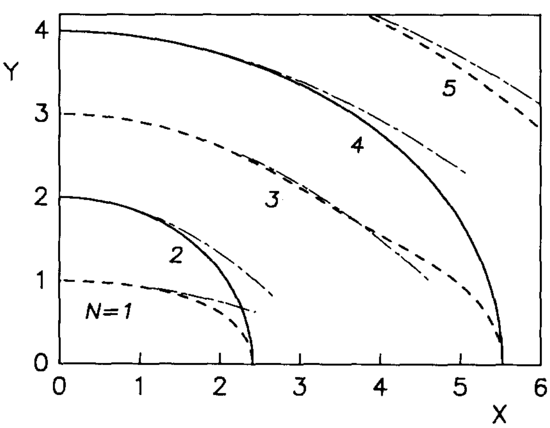

Fig. 2. Generalized Bloch–Siegert resonance curves for both odd-N (dashed) and even-N Haroche resonances (solid), obtained in the limit of zero damping (see ref. [8]). The lowest-order shifts from eq. (4) are indicated by the thin lines. The coordinates X and Y are defined in table 1. The limiting behaviors are given by $Y=N$ for $X=0$ ("multiple quantum resonances") and by $J_0(X)=0$ for $Y=0$ ("subharmonic resonances").

Table 1
Definitions of the coordinates X and Y in fig. 2 for the torques $\boldsymbol{R}$ defined in the text [eqs. (2), (6), (7), (3) and (9), respectively]

	odd-N			even-N	
$\boldsymbol{R}$	$\boldsymbol{R}_{\mathrm{mag}}^{\parallel}$	$\boldsymbol{R}_{\mathrm{opt}}^{\mathrm{C}}$	$\tilde{\boldsymbol{R}}_{\mathrm{opt}}^{\mathrm{FAM}}$	$\boldsymbol{R}_{\mathrm{mag}}^{\perp}$	$\tilde{\boldsymbol{R}}_{\mathrm{opt}}^{\mathrm{RPM}}$
X	$\omega_{\mathrm{rf}}/\Omega$	$2\kappa\mathscr{E}/\omega$	$\kappa\mathscr{E}/\Omega$	$\omega_{\mathrm{rf}}/\Omega$	M
Y	ω_0/Ω	ω_{12}/ω	Δ/Ω	ω_0/Ω	$\kappa\mathscr{E}/\Omega$

3. Optical Haroche and Hanle resonances

Both the Haroche and Hanle resonances can be computed by developing the Bloch vector $\Phi(t)$ from eq. (5) as a Floquet series:

$$\Phi(t) = \sum_{k=-\infty}^{\infty} (u_k, v_k, w_k) \exp(\mathrm{i}k\Omega t) , \tag{10}$$

and solving for the coefficients u_k, v_k and w_k in terms of scalar continued fractions [5]. Specifically, if we introduce the polarization and population decay rates $\Gamma_1 = \Gamma_2 = T_2^{-1}$ and $\Gamma_3 = -\Lambda_{\mathrm{opt}} = T_1^{-1}$, and define the factors $b_k^{(j)} = 1 + \mathrm{i}k\Omega T_j$ ($j = 1, 2$), eqs. (5), (9) and (10) yield the recurrence relations

$$b_k^{(2)} u_k = -\tfrac{1}{2} M\Omega T_2 (v_{k+1} + v_{k-1}) , \tag{11a}$$

$$b_k^{(2)} v_k = \tfrac{1}{2} M\Omega T_2 (u_{k+1} + u_{k-1}) + \kappa\mathscr{E} T_2 w_k , \tag{11b}$$

$$b_k^{(1)} w_k = -\kappa\mathscr{E} T_1 v_k - \delta_{k0} . \tag{11c}$$

Eliminating the w_k's and observing that $u_k=0$ for k=even and $v_k=0$ for k=odd, eqs. (11) can be combined into a single recurrence relation for the coefficients

$$\psi_k = u_k\,, \quad k=\text{odd}\,,$$
$$= v_k\,, \quad k=\text{even}\,, \tag{12}$$

namely

$$(-1)^{k+1} B_k \psi_k + \mathcal{M}^{1/2}(\psi_{k+1}+\psi_{k-1}) = \kappa\mathscr{E} T_2 \delta_{k0}\,, \tag{13}$$

where

$$B_k = b_k^{(2)}\,, \qquad k=\text{odd}\,,$$
$$= b_k^{(2)} + I/b_k^{(1)}\,, \quad k=\text{even}\,, \tag{14}$$

and where we have introduced the dimensionless modulation rate $\mathcal{M}=\frac{1}{2}M\Omega T_2$ and the dimensionless intensity $\mathscr{I}=(\kappa\mathscr{E})^2 T_1 T_2$. Introducing, furthermore, the factors

$$S_k = (-1)^k \mathcal{M}^{1/2}(\psi_k/\psi_{k-1})\,, \tag{15}$$

eq. (13) becomes, upon dividing by $(-1)^k\psi_k$,

$$-B_k - S_{k+1} + \mathcal{M}/S_k = (\kappa\mathscr{E} T_2/v_0)\,\delta_{k0}\,. \tag{16}$$

Thus, for $k\geqslant 1$, the S_k's are given by scalar continued fractions, namely by backward recursion of

$$S_k = \mathcal{M}/(B_k + S_{k+1})\,. \tag{17}$$

Since $B_{-k}=B_k^*$, eq. (16) implies that, for $k\geqslant 1$, $S_k = -\mathcal{M}/S^*_{-k+1}$, and that, specifically, $\mathcal{M}/S_0 = -S_1^*$. Thus, eq. (16) yields, for $k=0$:

$$v_0 = \frac{-\kappa\mathscr{E} T_2}{1+\mathscr{I}+2\,\mathrm{Re}\{S_1\}}\,, \tag{18}$$

where we have used $B_0 = 1+\mathscr{I}$. For $k=0$, eq. (11c) gives $1+\omega_0 = -\kappa\mathscr{E} T_1 v_0$ so that, finally, the time-averaged population inversion $\rho_{22}^{(0)}$ is given by

$$\rho_{22}^{(0)} = \tfrac{1}{2}(1+\omega_0) = \tfrac{1}{2}\mathscr{I}/(1+\mathscr{I}+2\,\mathrm{Re}\{S_1\})\,. \tag{19}$$

For zero modulation, $S_1=0$, and $\rho_{22}^{(0)}$ follows a simple saturation curve as a function of the intensity $\mathscr{I}$. However, as the modulation index M increases, two new effects become manifest, as is illustrated in fig. 3: These are the Haroche and Hanle resonances.

As in magnetic resonance, the Hanle effect determines the behavior of $\rho_{22}^{(0)}$ for small fields. Indeed, in fig. 3, the behavior of the curves at the origin depends greatly on the modulation index M. It may be shown that, for weak fields and small damping, $\rho_{22}^{(0)} \simeq \frac{1}{2}\mathscr{I} J_0^2(M)$. Thus, the slow rise of the curve with $M=2.4$ in fig. 3 is explained by the vanishing of the J_0-Bessel function. This effect is analogous to the dressing of the atomic Landé factor in magnetic resonance [4].

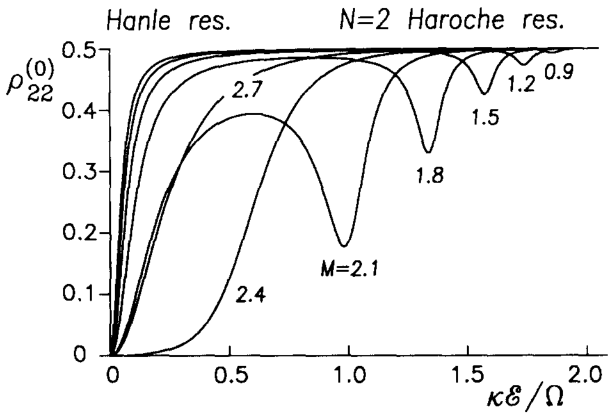

Fig. 3. Time-averaged upper state population as a function of the scaled electric field, for various values of the modulation index M ($\Omega T_1 = \Omega T_2/2 = 20$). The optical Hanle and Haroche resonances occur for $\kappa\mathscr{E}\simeq 0$ and $\kappa\mathscr{E}\lesssim 2\Omega$, respectively.

Similarly, in fig. 3, the Haroche resonances manifest themselves as dips in the saturated values of $\rho_{22}^{(0)}$ near $\kappa\mathscr{E}=N\Omega$, with $N=2, 4, 6, \ldots$. For weak modulation, the positions of the resonances are given by the expressions for the weak-field Bloch-Siegert shifts from eq. (4). For example, the $N=2$ resonance is located at $\kappa\mathscr{E}/\Omega \simeq 2 - M^2/6$. In general, the resonances shift along the solid curves in fig. 2. Thus, the $N=2$ resonance disappears for $M\simeq 2.4$, as it merges with the Hanle resonance.

The Haroche resonances are also present in modulated components of $\rho_{22}(t)$, the lowest nonvanishing of which is modulated at 2Ω. In terms of the scalar continued fractions S_k above, its complex amplitude is given by

$$\rho_{22}^{(2)} = \tfrac{1}{2}\omega_2 = -\rho_{22}^{(0)}(S_1 S_2/\mathcal{M} b_2^{(1)})\,, \tag{20}$$

which follows from eq. (11c) (with $k=2$), eq. (15) (yielding $v_2 = -v_0 S_1 S_2/\mathcal{M}$), and eqs. (18) and (19). For small M, small damping, and $\kappa\mathscr{E}\simeq 2\Omega$, eq. (20) may be approximated by

$$\rho_{22}^{(2)} \simeq \frac{\mathrm{i}M^2/32T_1}{\kappa\mathscr{E}-2\Omega+\frac{1}{6}M^2\Omega+\mathrm{i}\Gamma}, \qquad (21)$$

where $2\Gamma=T_1^{-1}+T_2^{-1}$. Thus, even for small M, $\rho_{22}^{(2)}$ displays clearly the $N=2$ Haroche resonance, namely as an absorptive (dispersive) feature in the real (imaginary) component, respectively. This resonance is shifted by the same amount as the corresponding dip in the time-averaged component, and is unbroadened to lowest orders in the modulation index and field strength. Similar results can be obtained for components of $\rho_{22}(t)$ modulated at 4Ω, 6Ω, etc., and for resonances with $N>2$.

4. Experimental realization

To show that the Haroche resonances should indeed allow the observation of an optical Bloch–Siegert shift, we assume an experiment as that used by Grove et al. to measure the Mollow fluorescence spectrum [11]. Thus, a narrowly collimated beam of sodium atoms is prepared as a two-level system by optical pumping. Furthermore, we assume that a narrowband ($\lesssim$ 1 MHz) dye laser, tuned to the 3 $^2S_{1/2}$ $(F=m_F=2)-3\,^2P_{3/2}$ $(F'=m'_F=3)$ transition, is phase-modulated by passage through a $LiTaO_3$ crystal, driven at, say, $\Omega/2\pi=300$ MHz and yielding a modulation index $M=0.8$ (values up to 3.2 have been achieved [12]). The resulting shift, $\delta_{BS}=\frac{1}{6}M^2\Omega/2\pi=32$ MHz, thus exceeds the natural linewidth, $(2\pi T_1)^{-1}=10$ MHz. To achieve a Rabi frequency $\kappa\mathscr{E}\simeq 2\Omega$, a peak irradiance of 45 W/cm^2 is needed. For a 20 mW, TEM_{00} beam, this calls for a spot size (radius at which the intensity drops by e^{-2}) $w_0=0.1$ mm. This spot size allows an interaction region of reasonable length, say $L=2$ mm, without causing significant Doppler broadening due to wavefront curvature. However, it is too small to allow comfortable imaging of a region with small intensity variations. But unlike the three-peak Mollow spectrum [11] and the two-peak Autler–Townes doublet [13], the single-peak Haroche resonances may be observed – at the position given by the Bloch-Siegert shift – even if the (modulated) signal is integrated over the beam cross-section. Indeed, fig. 4 shows the TEM_{00}-averaged absorption/emission signal $\mathscr{R}^{(2)}$ at twice the modulation frequency, which is given by

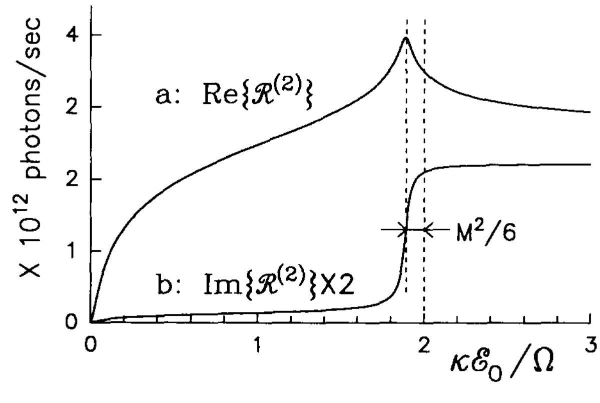

Fig. 4. In-phase (a) and quadrature (b) components of the modulated, TEM_{00}-averaged absorption/emission signal $\mathscr{R}^{(2)}$ from eq. (21) versus the scaled peak Rabi frequency, for $M=0.8$ and $\Omega T_1=\Omega T_2/2=30$. The vertical scale corresponds to $w_0=0.1$ mm, $L=2$ mm, $(2\pi T_1)^{-1}=10^7\ s^{-1}$, and $n_a=3.75\times10^9\ cm^{-3}$.

$$\mathscr{R}^{(2)}=(\pi w_0^2 L n_a/T_1)\int_0^{\mathscr{E}_0} b_2^{(1)}\rho_{22}^{(2)}(\mathscr{E})\,\frac{\mathrm{d}\mathscr{E}}{\mathscr{E}}, \qquad (21)$$

where $\mathscr{E}_0$ is the peak electric field, and n_a is the density of atoms in the interaction region. Fig. 4 shows that the in-phase and quadrature components of $\mathscr{R}^{(2)}$ clearly display a resonance-feature and a step-feature at the shifted peak Rabi-frequency $\kappa\mathscr{E}_0=2\Omega-M^2/6$. For the parameters indicated ($n_a=\frac{5}{8}\times6\times10^9$ atoms/cm^3 [11]), the modulated photon flux is of the order of $4\times10^{12}\ s^{-1}$, corresponding to an average power of 1 µW. Using a fast photodetector, this signal may be selectively amplified by homodyning in a double balanced mixer, which is referenced to the frequency-doubled output from the radiofrequency driver of the modular crystal [12].

Although, in a detailed analysis, such effects as residual Doppler broadening [#1] and other experimental artifacts may be taken into account, we conclude that the prospects for the measurement of an optical Bloch–Siegert shift are quite good. In fact, to merely observe the Haroche (and Hanle) resonances, that is, without measurement of their shift, many of the above parameters and constraints may be relaxed significantly, thereby yielding a much easier experiment. Beyond the proof-of-principle experiments, the narrow Haroche resonances may find applica-

[#1] To solve eqs. (5) and (9) for $\Delta\neq0$ see ref. 1, and ref. [14].

tions in the evolving field of phase- and frequency-modulation spectroscopy [15].

5. Summary

It is shown that there exists a full analogy between magnetic and optical resonance experiments involving modulated fields, wherein the role of optical pumping in the magnetic regime is replaced by amplitude- or phase-modulation in the optical regime. Specifically, it is shown that resonant excitation of a two-level atom with a narrow-band, phase-modulated laser produces the optical equivalents of Haroche and Hanle resonances. It is also calculated that, for a specific system, namely sodium, the Haroche resonances should allow the first observation of an optical Bloch-Siegert shift.

Acknowledgement

This research was supported by the Centers of Excellence Program of the Tennessee Higher Education Commission.

References

[1] W.M. Ruyten, Phys. Rev. A 40 (1989) 1447;
W.M. Ruyten, J. Opt. Soc. Am. B 6 (1989) 1796;
W.M. Ruyten, Optics Lett. 14 (1989) 506.

[2] W.M. Ruyten, Phys. Rev. A39 (1989) 442.

[3] W. Hanle, Z. Phys. 30 (1924) 93; for a discussion of the optical Hanle effect in a different context see: P. Anantha Lakshmi and G.S. Agarwal, Phys. Rev. A23 (1981) 2553.

[4] C. Cohen-Tannoudji, in: Cargèse Lectures in Physics, Vol. 2, ed. M. Lévy (Gordon and Breach, New York, 1968) p. 347;
C. Cohen-Tannoudji and S. Haroche, Comptes Rendus 261 (1965) 5400;
S. Haroche, Ann. Phys. Paris 6 (1971) 189, 327.

[5] S. Stenholm and C.-G. Aminoff, J. Phys. B: At. Mol. Phys. 6 (1973) 2390;
see also S. Stenholm, J. Phys. B: At. Mol. Phys. 5 (1972) 878, 890; 6 (1973) 1097.

[6] T. Yabuzaki, N. Tsukada and T. Ogawa, J. Phys. Soc. Jpn. 33 (1972) 698;
N. Tsukada and T. Ogawa, J. Phys. B: At. Mol. Phys. 6 (1973) 1643;
N. Tsukada, Y. Murakami and T. Ogawa, J. Phys. B: At. Mol. Phys. 6 (1973) 2605.

[7] C. Cohen-Tannoudji, J. Dupont-Roc and C. Fabre, J. Phys. B: At. Mol. Phys. 6 (1973) L218.

[8] S. Swain, J. Phys. B: At. Mol. Phys. 7 (1974) 2363.

[9] L. Allen and J.H. Eberly, Optical resonance and two-level atoms (Wiley, New York, 1975).

[10] S. Chakmakjian, K. Koch and C.R. Stroud, Jr., J. Opt. Soc. Am. B5 (1988) 2015.

[11] R.E. Grove, F.Y. Wu and S. Ezekiel, Phys. Rev. A15 (1977) 227.

[12] D.E. Cooper and T.F. Gallagher, Appl. Optics 24 (1985) 1327;
N.H. Tran, T.F. Gallagher, J.P. Watjen, G.R. Janik and C.B. Carlisle, Appl. Optics 24 (1985) 4282.

[13] J.L. Picqué and J. Pinard, J. Phys. B: At. Mol. Phys. 9 (1976) L77;
H.R. Gray and C.R. Stroud, Jr., Optics Comm. 25 (1978) 359.

[14] N. Nayak and G.S. Agarwal, Phys. Rev. A 31 (1985) 3175.

[15] G.C. Bjorklund, Optics Lett. 5 (1980) 15;
A. Schenzle, R.G. DeVoe and R.G. Brewer, Phys. Rev. A 25 (1982) 2606.